

Syntheses, Photophysical Properties, and Application of Through-Bond Energy-Transfer Cassettes for Biotechnology

Guan-Sheng Jiao,^[a] Lars H. Thoresen,^[a] Taeg Gyum Kim,^[b] Wade C. Haaland,^[c] Feng Gao,^[b] Michael R. Topp,^[b] Robin M. Hochstrasser,^[b] Michael L. Metzker,^[c] and Kevin Burgess^{*[a]}

Abstract: We have designed fluorescent “through-bond energy-transfer cassettes” that can harvest energy of a relatively short wavelength (e.g., 490 nm), and emit it at appreciably longer wavelengths without significant loss of intensity. Probes of this type could be particularly useful in biotechnology for multiplexing experiments in which several different outputs are to be observed from a single excitation source. Cassettes **1–4** were designed, prepared, and studied as model systems to achieve this end. They were synthesized through convergent routes that feature coupling of specially prepared fluorescein- and rhodamine-derived

fragments. The four cassettes were shown to emit strongly, with highly efficient energy transfer. Their emission maxima cover a broad range of wavelengths (broader than the four dye cassettes currently used for most high-throughput DNA sequencing), and they exhibit faster energy-transfer rates than a similar through-space energy-transfer cassette. Specifically, energy-transfer rates in these cassettes is

around 6–7 ps, in contrast to a similar through-space energy-transfer system shown to have a decay time of around 35 ps. Moreover, the cassettes are considerably more stable to photobleaching than fluorescein, even though they each contain fluorescein-derived donors. This was confirmed by bulk fluorescent measurements, and in single-molecule-detection studies. Modification of a commercial automated DNA-sequencing apparatus to detect the emissions of these four energy-transfer cassettes enabled single-color dye-primer sequencing.

Keywords: cross-coupling • DNA • dyes/pigments • fluorescence resonance energy transfer • fluorescent probes

Introduction


Multiplexing of fluorescent labels is a common requirement in biotechnology. Often, one laser excitation source is available to stimulate emissions from several dyes on different biomolecules. One problem with this approach is that the requirements for resolution and sensitivity are opposing. Good resolution requires that the fluorescence emissions be well spaced over a range of wavenumbers. However, high sensitivity requires good overlap of the absorption spectra with the excitation source, which is difficult to achieve if dyes are modified so that they fluoresce further towards the red.

Perhaps the best-known example of multiplexing in biotechnology is the Sanger sequencing^[1,2] of DNA, a methodology that illustrates well the principles and challenges of multiplexing. Current methodologies for high-throughput DNA sequencing use fluorescence detection of the chain-terminated fragments.^[3–5] Four fluorescent labels are required, corresponding to termination with ddATP, ddTTP,

[a] Dr. G.-S. Jiao, Dr. L. H. Thoresen, Prof. K. Burgess
Department of Chemistry, Texas A & M University
P.O. Box 30012, College Station, Texas 77842 (USA)
Fax: (+1) 979-845-8839
E-mail: burgess@tamu.edu

[b] Dr. T. G. Kim, Dr. F. Gao, Prof. M. R. Topp, Prof. R. M. Hochstrasser
Department of Chemistry, University of Pennsylvania
Philadelphia, PA 19104 (USA)

[c] W. C. Haaland, Prof. M. L. Metzker
Department of Molecular and Human Genetics
Baylor College of Medicine, Houston, TX 77030 (USA)

 Supporting information for this article is available on the WWW under <http://www.chemeurj.org/> or from the author: Syntheses of compounds **1–4**, absorption and fluorescence spectra of compounds **1–4**, tabulated spectroscopic properties of compounds **1–4**, details of the Sanger sequencing experiments.

ddGTP, and ddCTP. Ideally, the fluorescence outputs from these four labels should be intense, sharp, and well resolved, as shown in the hypothetical situation in Figure 1a.

In practice, the ideal fluorescence signals shown in Figure 1a cannot be obtained by using any of the dye sets currently available for sequencing with single-laser systems. Typically, the resolution is satisfactory, but the intensity of the signals diminishes as the emission wavelengths become longer (Figure 1b). This has the effect that identification (“calling”) of the labeled chain-terminated fragments becomes more diffi-

cult, effectively establishing an upper limit to the number of bases that can be sequenced in a single experiment.

The origin of the diminished red-fluorescence signals is related to the fact that nearly all the automated sequencing machines use only one laser excitation source.^[4,6] If this source operates at 488 nm, then a dye with a high extinction coefficient at this wavelength will absorb photons efficiently, and emit strongly. Typically, this is true for the dye that emits with the shortest wavelength, the one that might be called the *blue* dye (Figure 1c). Conversely, the dye that emits at the longest wavelength (the *red* dye) will have the smallest extinction coefficient at 488 nm. It will absorb photons least effectively and will emit less intensely than the blue dye. This reasoning assumes that the quantum yields of the two dyes are similar, and for the fluorescein/rhodamine systems that are typically used, this is realistic.

State-of-the-art dyes for high-throughput DNA sequencing^[7–12] use fluorescence resonance energy transfer (FRET)^[13] to enhance the signals from the red dyes. FRET systems for DNA sequencing use pairs (or even more than two, see below) of dyes to perform the job normally done by one sequencing dye. Four distinct pairs of dyes are used, one pair for each termination reaction. One dye, called the *donor*, is common to all pairs. It functions to absorb photons efficiently at the excitation wavelength, then relays the energy to the second dye in the pair. The second dye, the *acceptor*, accepts the energy relayed to it through resonance with the donor (and any that it can absorb from the excitation source), then emits at its characteristic fluorescence wavelength. Originally, the donor and acceptor dyes were attached to different DNA bases in the oligonucleotide primers used for sequencing.^[7,14–26] The currently preferred approach is to incorporate the donor and acceptor dyes into one molecular entity that can be coupled to a nucleoside base (either in the primer or to the dideoxynucleotide triphosphate terminator) in one conjugation reaction.^[9,10,27,28] Hereafter, we refer to such systems as through-space energy-transfer cassettes, because the energy transfer (Förster) occurs through space. The structures of the latest generations of through-space energy-transfer cassettes are not readily deduced from the literature,^[7,22,29] but they are probably similar to the typical Applied Biosystems^[9–11] and Amersham^[27,28] structures **A** and **B**, and derivatives of these.

The extent of through-space energy transfer possible in cassettes is limited by the physics of FRET.^[13] A key parameter in FRET is “the overlap integral”; this crudely represents overlap of the fluorescence emission of the donor with the absorption of the acceptor, even though the donor does not actually transfer energy in the form of fluorescence. If a donor is designed to harvest photons at a particular wavelength, an acceptor with a strong absorption at an appropriate wavelength must be chosen if FRET is to be efficient; this excludes acceptors that absorb and emit at much longer wavelengths. It is possible to use three dyes, rather than two, to extend the wavelength difference between the donor absorption and the acceptor emission,^[30–34] however, such systems are more difficult to construct, they alleviate the con-

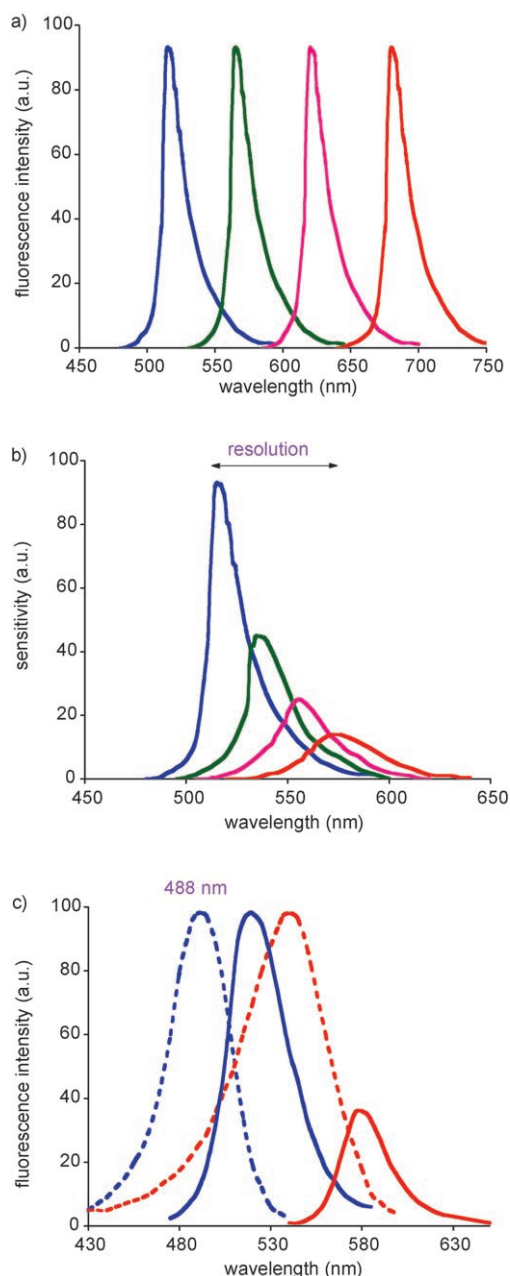


Figure 1. a) Idealized fluorescence emissions from dyes used in DNA sequencing. b) An approximate representation of data obtained from single dyes in DNA sequencing. c) Diminished fluorescence intensities of the red dyes can be attributed to their lower extinction coefficients at the excitation wavelength, relative to the blue dyes.

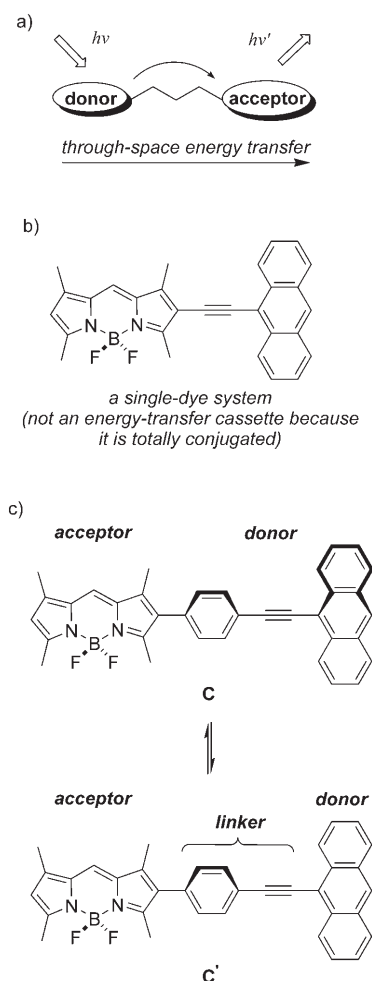
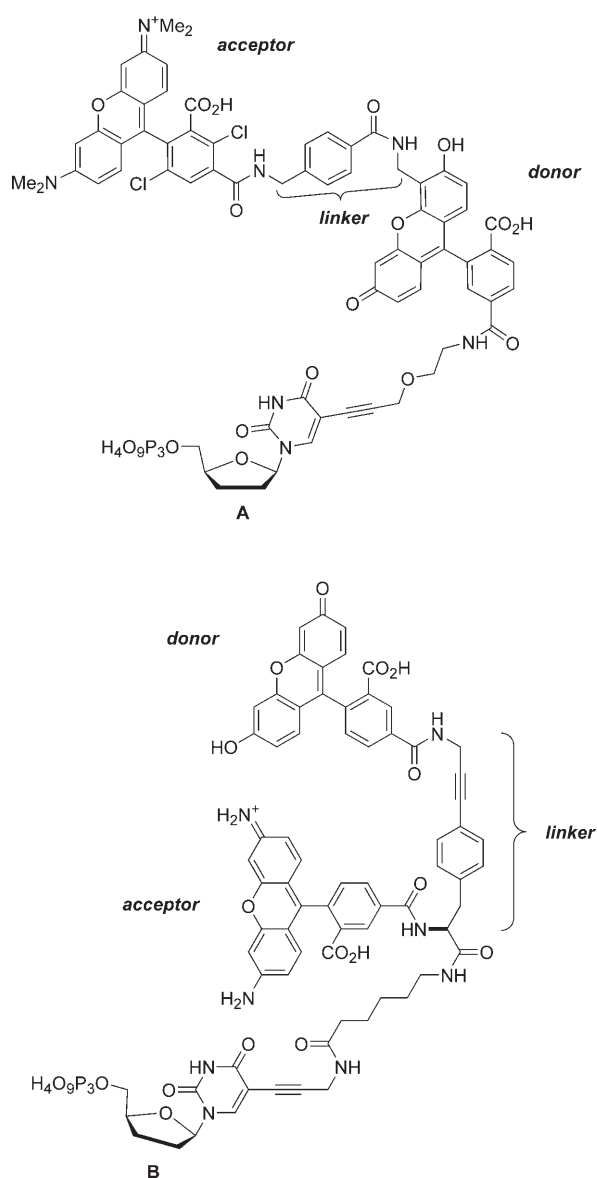


Figure 2. a) A generic through-space energy-transfer cassette. b) Conjugated, planar donor and acceptor fragments do not produce energy-transfer cassettes. c) Donor and acceptor fragments linked by conjugated systems that do not allow them to become planar can act as energy-transfer cassettes; **C** and **C'** are major contributing conformations.

straint only partly, and there are other disadvantages associated with the bulk of molecules containing three dyes.

Our interest in this area is to construct dyes that would facilitate mechanisms of energy transfer other than FRET. If these mechanisms are not constrained by parameters, such as the overlap integral, then it will be necessary to reevaluate the limits of the wavelength difference between the donor absorption and the acceptor emission.

Clues hinting at other energy-transfer mechanisms that could be harnessed to make energy-transfer cassettes came initially from research on materials chemistry^[35–38] and photosynthetic models,^[39–42] then from model compounds of our own.^[43–45] Importantly, all the through-space energy-transfer cassettes prepared for biotechnology had featured donor and acceptor entities *linked by molecular fragments that do not allow any possibility of conjugation between the donor and acceptor parts* (Figure 2a). Conversely, molecules having

donor and acceptor fragments linked through unsaturated molecular species that allow them to become planar are unlikely to act as energy-transfer systems, because the donor and acceptor parts become electronically conjugated to form new, extended chromophores (Figure 2b). However, if donor and acceptor entities are joined through a conjugated linker that prevents the two parts from becoming planar, then a *through-bond energy-transfer cassette* results (Figure 2c). As for the corresponding through-space energy-transfer systems, through-bond energy-transfer cassettes are characterized by UV-absorption spectra that closely resemble the sum of their donor/linker/acceptor parts, whereas the fluorescence of the donor is suppressed, and the corresponding emission of the acceptor is enhanced. The key difference is that the linker is unsaturated and steric constraints prevent the whole molecule from becoming planar. The structure-based design of such systems to harness through-bond energy-transfer mechanisms involving dyes for biotechno-

logical applications was an unforeseen development in this field.

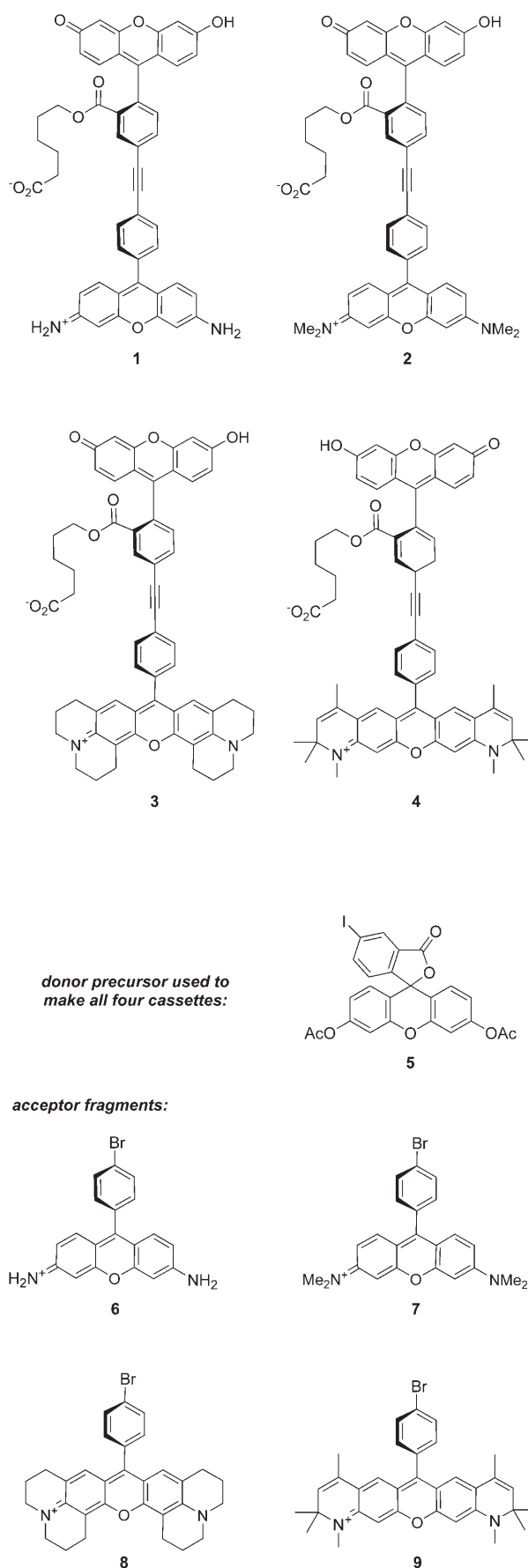
Through-bond energy transfer is not constrained by the same parameters as the corresponding through-space mechanisms. Thus, there is no parameter similar to the overlap integral (overlap of the donor fluorescence with the acceptor absorbance) that limits through-space energy transfer by the Förster mechanism. It may, therefore, be possible to separate the donor absorption from the acceptor fluorescence by many wavenumbers without compromising the intensity of the light emitted. This potential for enhanced resolutions without loss of sensitivity is an important motivation for developing these through-bond energy-transfer cassette systems.

Energy-transfer cassettes designed to transfer energy through bonds will always transfer a certain component of the energy through space as well. Unfortunately, it is extremely difficult to ascertain the relative importance of the two pathways for smaller molecules. This is because some of the critical parameters that are used to estimate through-space energy transfer, Förster radii,^[46] cannot be measured, and must be estimated. The extent of energy transfer is dependent on Förster radii raised to the sixth power, so application of Förster theory to molecules in which the donor and acceptor parts are too close to measure accurately is extremely imprecise.

In preliminary work, we communicated the preparations and basic photophysical properties of cassettes **1–4**.^[47] These systems are designed to harness through-bond energy transfer for biotechnological applications. Here, we expand on these studies in several important respects. Firstly, details of improved synthetic schemes to obtain these molecules are reported. Secondly, the basic photophysical properties of these molecules are compared with data from ultrafast dynamic spectroscopic studies to attempt to quantitate the rate and extent of energy transfer between the donor and acceptor components. These studies cannot show exact ratios of through-space and through-bond energy transfer, but they can be used to determine if both pathways are operative. Finally, experiments to determine if cassettes **1–4** can be used in PCR and sequencing reactions were performed.

Results and Discussion

Syntheses of the cassettes: Milestones in the preparation of the cassettes were the development of routes to some key starting materials; 5-iodofluorescein diacetate **5** (a synthon for the donor parts) and the rhodamine derivatives “rosamines” **6–9** (the acceptor precursors). The purpose of using acceptor components lacking a carboxylic acid functionality was that regioselectivity issues would not arise upon attachment of the cassettes. Consequently, the rosamines **6–9** were selected instead of rhodamines, which have this substituent on the phenyl ring. A practical, multigram scale procedure to obtain the 5-iodofluorescein diacetate **5** developed for this project has been reported.^[48] The rosamines **6–9** were



prepared by means of thermal condensation reactions. Procedures for these reactions that rely on conventional heating are given in the Supporting Information, however, we have also reported expedient alternatives involving microwave heating.^[49]

The syntheses of cassettes **1–4** were designed to proceed via a common advanced intermediate that could then be coupled with four different acceptor fragments. Thus, the fluorescein derivative **5** was transformed into the key fluorescein alkyne **12** by the route shown in Scheme 1. This involved the Sonogashira reaction followed by deprotection and finally esterification.

From intermediate **12**, each of the cassettes could be prepared by using the two-step procedure outlined in Scheme 1a. This involved a Sonogashira coupling, then deprotection of the *tert*-butyl ester. Cassettes **1–4** were isolated as brightly colored solids (orange, maroon, dark green, and dark blue, respectively). These cassettes have the same fluorescein-based donor fragment, but variable acceptor parts based on the rosamine fragments **6–9**.

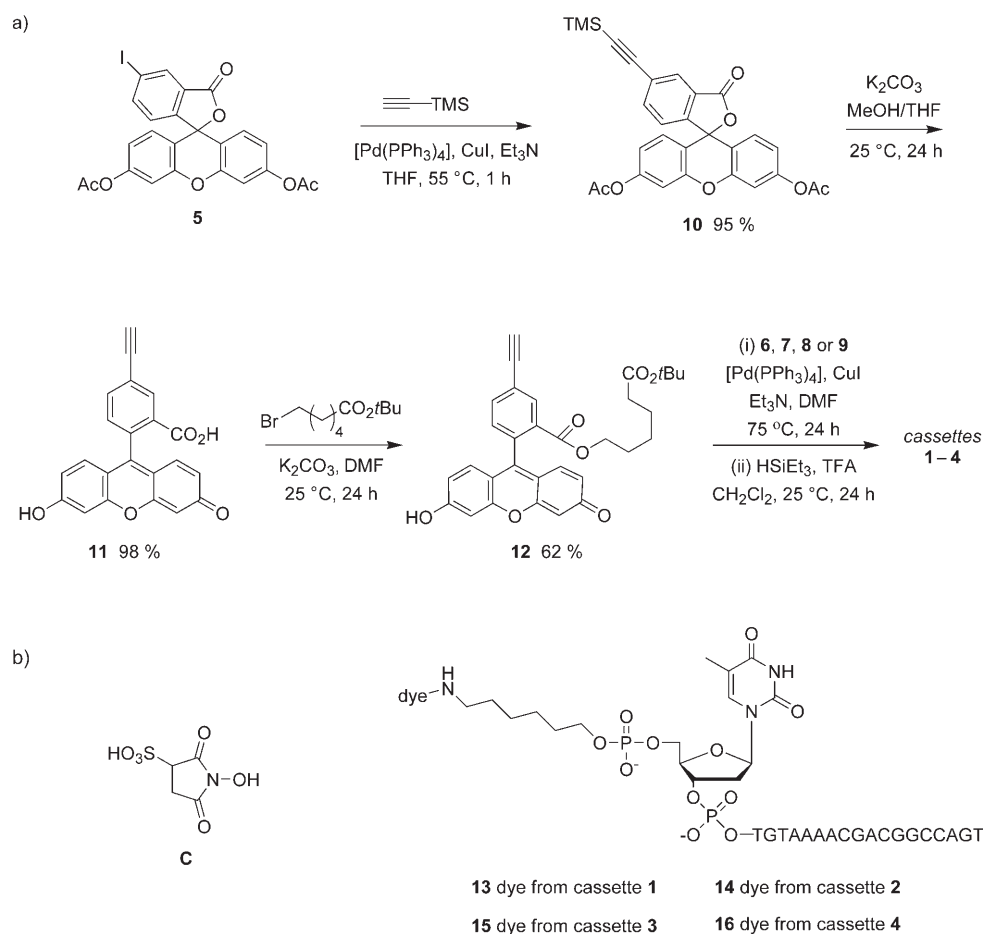
The cassettes are not very soluble in water. Consequently, they were functionalized with the *N*-hydroxysulfosuccinimide **C** (Scheme 1b) to activate the ester for bioconjugation;

the resulting derivatives, such as **13**, have enhanced water solubilities. Without isolation, these activated ester intermediates were then reacted with amine-functionalized oligonucleotides in aqueous organic media (see Supporting Information) to give the water-soluble, cassette-labeled oligonucleotide primers **13–16**^[16] (Scheme 1b).

Photophysical properties of the cassettes

Various spectroscopic techniques were used to assess the photophysical properties of cassettes **1–4**, including straightforward absorption and fluorescence measurements, fluorescence quantum yield determinations, and ultrafast time-resolved fluorescence techniques to measure energy-transfer rates.

UV-absorption and fluorescence-emission spectra of the cassettes: Figure 3a shows the absorption spectra of the cassettes in “absolute” ethanol, which has sufficient basicity to allow deprotonation of the fluorescein chromophore. Alternatively, one could achieve the same results by adding small amounts of basic buffer to pure ethanol solutions. All the cassettes have a strong absorption band close to 500 nm cor-



Scheme 1. a) Synthesis of the donor synthon **12**. b) Structure of the *N*-hydroxysulfosuccinimide **C** and the cassette-labeled oligonucleotide primers **13–16**.

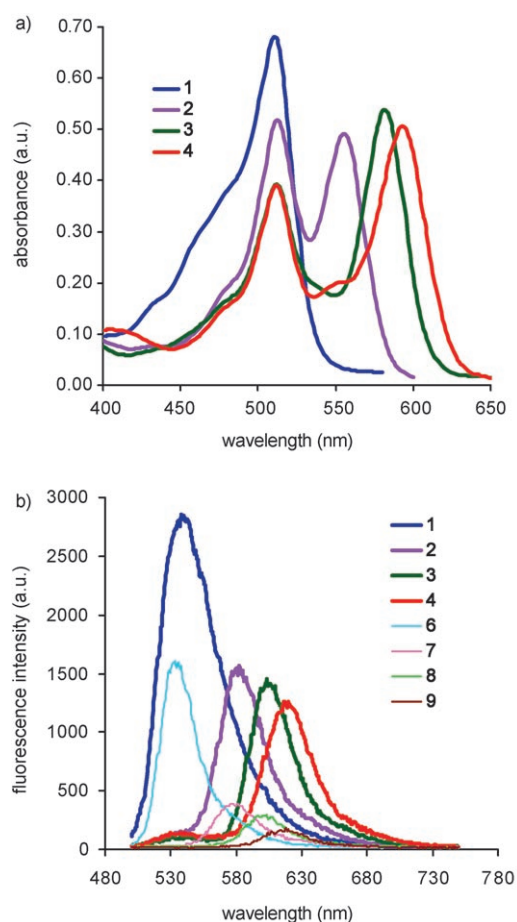


Figure 3. a) Absorption and b) emission spectra of equimolar solutions of the cassettes **1–4** in absolute ethanol. **6–9** are the acceptor fragments.

responding to the λ_{max} of the fluorescein donor component, present as the dianion. Cassettes **3** and **4** have almost identical extinction coefficients at this wavelength, reflecting the fact that the acceptor parts of these molecules absorb weakly at this wavelength (see Supporting Information for absorption spectra of the acceptor analogs **6–9**). However, this is not the case for cassettes **1** and **2**. The acceptor fragments of these molecules have significant absorptions close to 500 nm, and this is observed for the cassettes incorporating them. Cassettes **2–4** have clearly longer-wavelength absorption maxima that correspond to the absorption spectra of the acceptor parts. Overall, the absorption spectra closely resemble those that would be expected by summation of the donor and acceptor parts for each cassette.

Figure 3b shows the fluorescence spectra of the cassettes, and of the acceptor fragments **6–9**, in absolute ethanol. The Big Dyes currently used for most high-throughput sequencing work cover the range spanned by cassettes **1–3**; the range covered by **1–4** is greater because the emission of cassette **4** is further towards the red than any of the acceptors used in the Big Dyes. For cassettes **3** and **4**, and less for **2**, there is some fluorescence in the range 530–550 nm, which is attributed to the presence of small amounts of impurities

(we were not able to remove these for practical reasons). Whatever the origin of this “residual donor fluorescence”, the data presented here indicate that the energy transfer within all the cassettes quenches the donor fluorescence very efficiently (>99%).

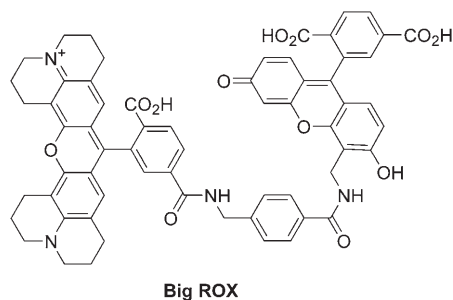
Steady-state quantum-yield determination: Although the relative fluorescence intensities of the four cassettes have been reported previously,^[47] we have extended the study here to compare the fluorescence intensities to standard values for fluorescein (0.79) and rhodamine 610 (1.0).^[50] The results are presented in Table 1.

Table 1. Quantum yields of energy-transfer cassettes and fragments in EtOH.

Sample	Excitation wavelength [nm]	Quantum yield
donor fragment 12a	490	0.61 ± 0.05
acceptor fragment 6	510	0.54 ± 0.05
acceptor fragment 7	540	0.66 ± 0.05
acceptor fragment 8	540	0.83 ± 0.03
acceptor fragment 9	540	0.52 ± 0.03
cassette 1	460	0.27 ± 0.03
cassette 1	490	0.29 ± 0.03
cassette 2	510	0.32 ± 0.03
cassette 2	550	0.32 ± 0.03
cassette 3	510	0.29 ± 0.03
cassette 3	565	0.27 ± 0.03
cassette 4	500	0.33 ± 0.03
cassette 4	550	0.36 ± 0.03
Big ROX	500	0.90 ± 0.02
Big ROX	550	0.91 ± 0.02

The fluorescence intensities of the different cassettes having similar absorbances were compared against the fluorescence standards, and corrected for small differences in sample absorption. Each cassette (except **4**) was excited at both the donor and acceptor absorption maxima for these measurements. The results in Table 1 show that, within the precision of the experiments, the quantum yield was the same for excitation of the donor or acceptor species, indicating that the efficiency of energy transfer is very high. The results also show that inclusion in the cassettes reduced the fluorescence quantum yield by about a factor of two relative to the isolated acceptor fragments. The Applied Biosystems Dye “Big ROX” also has a higher quantum yield than the present cassettes. This is probably due to the fact that rosamines have no acid substituent that restricts the rotation of the benzene ring attached to the heterocyclic core of the molecules, hence, more nonradiative loss of energy occurs due to a spinning of this substituent.

Ultrafast energy-transfer studies: The dynamics of energy transfer were monitored at a time resolution of ~150 fs by using a Ti:sapphire-based fluorescence upconversion apparatus.^[45,51] One reason for the choice of DNA-labeling cassettes involving fluorescein is that many labeling experiments have employed argon-laser radiation of wavelengths close to 500 nm for excitation. To optimize the excitation



conditions, we employed both the more routine excitation wavelength of 405 nm and a parametric amplifier (NOPA).^[52] The latter allowed precise excitation of the donor chromophore close to 500 nm, allowing us to select not only the site of electronic excitation in each cassette, but also to optimize the emission polarization. In this way, it was possible both to monitor the dynamics of energy transfer and to examine the anisotropy of both the donor and acceptor fluorescence signals. Apart from the excitation wavelength, the Ti:sapphire fluorescence upconversion apparatus was used in a standard way,^[53] feeding the output of a lock-in amplifier to a computer, which also controlled the optical delay line. Details of this apparatus will be given elsewhere, but it is significant to note that the width of the temporal response was ~ 150 fs (fwhm).

As noted above, some of the experiments used the second harmonic of Ti:sapphire laser at ~ 405 nm, which may be considered the “default” output. Although irradiation at this wavelength reached a higher excited singlet state of the donor species with some direct excitation of the acceptor, we found that the dynamics of donor–acceptor energy transfer did not vary significantly upon changing the excitation wavelength. On the other hand, as we show below, the fluorescence polarization anisotropy measurements required that the donor species be excited close to its absorption maximum close to 500 nm.

Figure 4a shows a sequence of gated emission spectra, recorded at three different times following excitation at 405 nm, for cassette **4** in ethanol. A clear evolution from donor (530 nm) to acceptor emission (640 nm) is apparent. Time evolutions of the emission monitored at fixed wavelengths of 550 and 610 nm are shown in Figure 4b. None of the traces, which were recorded for magic-angle polarization, fits a single-exponential model, although the dominant components tended to be around 3 ps. Weighted-average decay times are presented here because no detailed kinetic model is available. Notably, these numbers fell within a narrow range of 6–7 ps for the four cassettes. The energy-transfer rates in the “rosamine”–fluorescein cassettes are *at least ten times slower* than we reported earlier for the cassettes involving anthracene donors and dipyrrometheneboron difluoride (BODIPY) acceptors (< 200 –600 fs).^[45] These differences, and correlations with the orientation in each cassette of the donor and acceptor transition moments, are

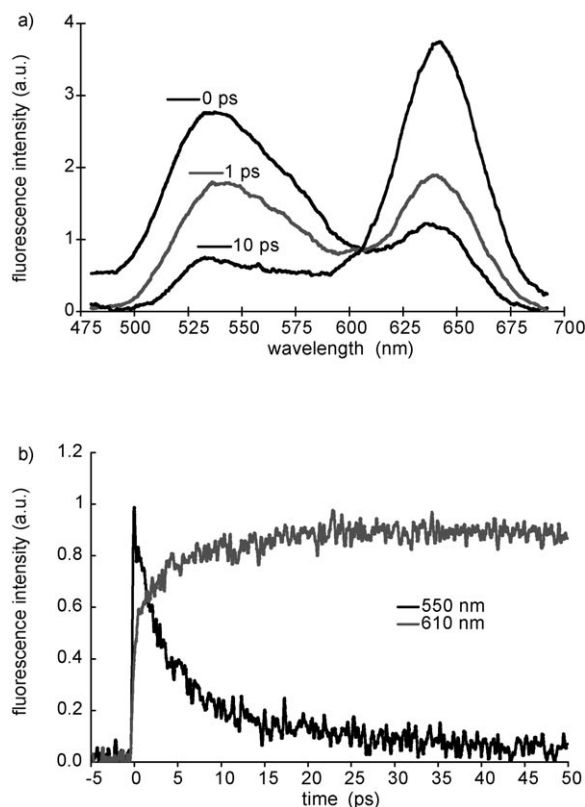


Figure 4. Energy transfer in cassette **4**. a) Time-resolved fluorescence spectra at three sampling times, showing the red shift of the emission spectrum. b) Fluorescence vs. time profiles at two sampling wavelengths.

significant for the interpretation of the energy-transfer mechanism, and will be discussed elsewhere.^[54] Similar experiments were performed on the species “Big ROX” by using 495 nm excitation and detection of both donor and acceptor emissions; the energy-transfer time was significantly longer than for the cassettes **1–4**, at ~ 35 ps. Because through-bond energy transfer is much less likely in this molecule, in which the donor and acceptor chromophores are linked by a sequence including single bonds, the measured rate essentially reflects the occurrence of FRET.

Because the absorption and fluorescence spectra of fluorescein are pH sensitive, we also varied the solvent conditions to investigate the quantum efficiency and rate of energy transfer. However, we found no significant differences in the overall fluorescence quantum yield in the pH range 7–10. On the other hand, there was a decrease in the donor fluorescence-decay time by about a factor of two upon dissolving the cassettes in a weakly basic buffer solution. This may reflect the known increase in the strength of the $S_1 \leftarrow S_0$ transition of fluorescein in basic solution^[55] and the consequent increase in coupling strength between the donor and acceptor chromophores.

Fluorescence anisotropy: We also measured the polarization anisotropy, $r(t)$, of the fluorescence within 50 ps of the exci-

tation pulse. During this short time, there is little molecular motion, and any depolarization effects following excitation of a defined transition are due to energy transfer. In brief, the anisotropy is calculated by using Equation (1), in which I_{\parallel} and I_{\perp} are the fluorescence intensities collected through a polarizer oriented parallel and perpendicular to, respectively, the plane of polarization of the exciting pulse:

$$r(t) = \frac{I_{\parallel} - I_{\perp}}{I_{\parallel} + 2I_{\perp}} \quad (1)$$

The maximum positive value of $r(t) = +0.4$ indicates that the absorption and fluorescence transitions are polarized exactly parallel to one another, and the maximum negative value of $r(t) = -0.2$ indicates that they are perpendicular.

These experiments employed excitation at 495 nm to achieve the greatest distinction between donor and acceptor excitation. This type of analysis requires that the absorbing transition is well characterized, which is most likely to be close to the maximum of the $S_0 \rightarrow S_1$ transition. This would not be true, for example, for excitation at 405 nm, at which there is a mixture of absorptions, due to different electronic states of both the donor and acceptor moieties. As may be expected, all donor species excited close to 500 nm showed an initial anisotropy of ≥ 0.3 , which is consistent with the model in which absorption and emission from the same state in a nonrotating molecule should fit the parallel case. However, the observation of nearly the same anisotropy, ≥ 0.25 , for the acceptor species in cassettes **1–4** indicates that the polarization is largely conserved during the energy transfer, and is good evidence for a structure in which the two xanthene ring systems are parallel. Thus, a consequence of exciting these cassettes with polarized light is that fluorescence of the acceptor species is also significantly polarized.

In contrast to the results described above, the dye Big ROX showed appreciable polarization only in the donor emission (i.e., $r(0) \sim r(t) \sim 0.33$), monitored at 510 nm, whereas the acceptor emission, monitored after 30 ps, was found to be unpolarized ($r(t) = 0 \pm 0.05$). This observation is consistent with a thermally averaged structure in which there is little orientational correlation between the donor and acceptor chromophores. This result reveals a potential advantage of the rigidly linked cassettes for labeling, as the polarized acceptor emission could provide an additional degree of selectivity, particularly if the molecular motion is restricted. For example, this could be a particular advantage of these rigidly linked cassettes in single-molecule studies, as the acceptor fluorescence shows appreciable polarization following excitation into the donor absorption maximum.

Photobleaching experiments: Fluorescein derivatives are notoriously prone to photobleaching, predominantly via triplet excited states.^[56] Cassettes **1–4** all contain fluorescein donors, so they too might be expected to be vulnerable to this mode of decomposition. In fact, they are considerably more stable to photobleaching than fluorescein itself (Figure 5). It may be that donor-to-acceptor energy transfer

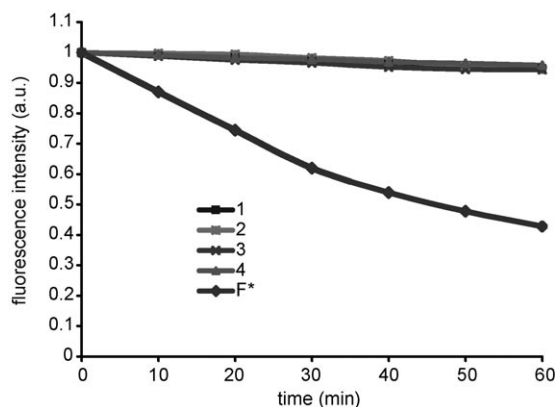
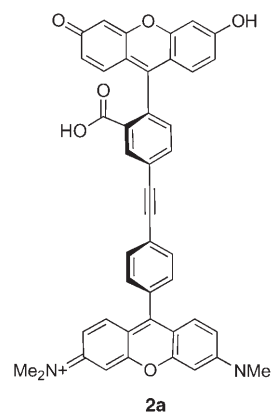


Figure 5. Photostabilities of cassettes **1–4** relative to fluorescein (F^*).

rates in **1–4** are so fast that intersystem crossing cannot compete, the triplet excited states of the donor are not significantly populated, energy is rapidly transferred to the rosamine parts that are intrinsically more stable to photobleaching, and the photostabilities of the cassettes are, therefore, greater than that of fluorescein.

Many researchers believe that high-throughput methods for sequencing DNA will eventually feature single-molecule detection methods. Photostabilities of dyes at the single-molecule level are, therefore, of considerable importance to these “futuristic” techniques. In work to be published elsewhere, we have shown that cassettes **1–4** have photostabilities that are comparable with rhodamine dyes *at the single-molecule level*. This implies that through-bond energy-transfer cassettes may be especially valuable in experiments that rely on detection of fluorescent labels at the single-molecule level.

Photobleaching characteristics of the cassette **2a** were studied by single-molecule fluorescence confocal microscopy.^[57] Results of these experiments found that under similar experimental conditions, cassette **2a** has photobleaching characteristics that are equally or even slightly more stable than the molecule corresponding to the acceptor part, that is, tetramethylrhodamine (TMR), in terms of the average survival time and the average number



of total photons emitted before photobleaching. For example, for excitation power $0.5 \mu\text{W}$ at 532 nm, the average survival time of **2a** is 12 s and the average number of total emitted photons is 46000. For TMR, the average survival time was 10 s and the average number of total counted photons was 18000. Figure 6 shows the data for **2a**, which is typical of all the samples.

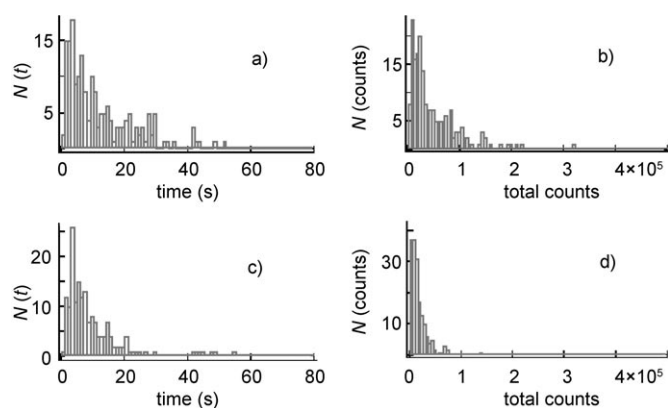


Figure 6. a) and c): Histograms of the survival times for single **2a** molecules and single TMR molecules, respectively. The count interval on the t axis is 1 s. b) and d): Histograms of the total photons detected by single **2a** molecules and TMR molecules, respectively. Excitation conditions: 0.5 μ W at 532 nm. N (counts) is the relative probability of measuring the indicated number of photon counts.

DNA-sequencing experiments: Cassettes **1–4** were coupled to the sequencing primer (R931, as in **13–16**) and were evaluated by using an ABI model 377 DNA sequencer. This four-color DNA sequencer uses an argon-ion laser (488 and 514.5-nm lines), which resolve fluorescent emission light by using a diffraction grating into blue, green, yellow, and red signals. These signals are imaged onto a charged-coupled device (CCD) camera. The CCD pixel array is divided into virtual color filters creating four collection windows, which are separated by nonimaged areas (Figure 7a). Virtual filters are programmed in the run-module software. To evaluate dye cassettes **1–4**, an alternative run module was created, which shifted the virtual collection windows to the red portion of the visible spectrum, corresponding to their emission maxima (Figure 7b). The range of the virtual windows was adjusted to maximize light collection for the four cassettes, while maintaining a minimum nonimage area of 12 nm (24 pixels) between the virtual filters.

Single-color, dye-primer Sanger sequencing reactions were carried out as described in the Experimental Section and were analyzed by using the modified run module on the 377 DNA sequencer. Figure 8 shows the single termination patterns of dye-primers **1–4** obtained by using automated DNA-sequencing instrumentation. The termination patterns were consistent with that of a corresponding nucleotide in the known DNA sequence. Attempts at analyzing the four dye-primer reactions in a single lane, as typically performed in four-color sequencing, however, proved challenging and did not yield typical DNA-sequence data (data not shown). The main obstacle here was our inability to create a working matrix file by using the manufacturer's DataUtility program. Among the numerous software steps required to transform "raw" data into "analyzed" data is the removal of spectral overlap or crosstalk between the dyes. We speculate that, although we successfully altered the run module for the detection of dye-primers from **1–4**, downstream-analysis programs may require additional modification before four-color

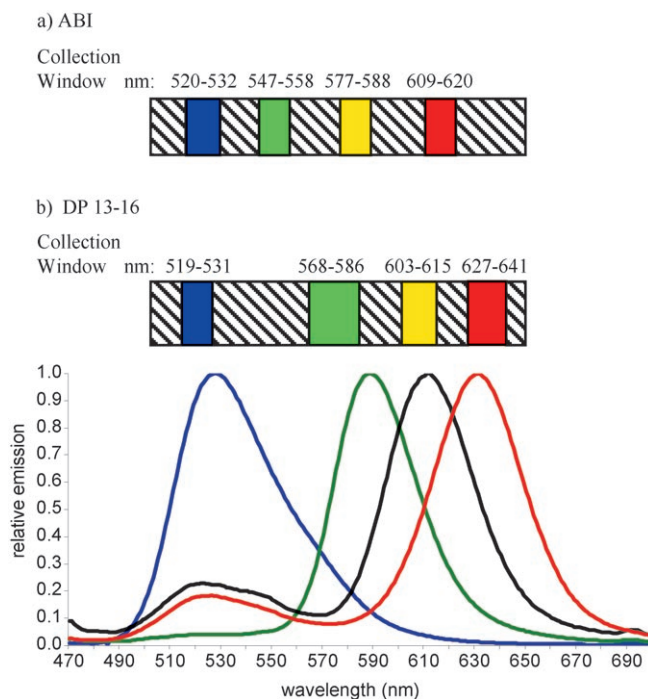


Figure 7. Schematic of the four virtual collection windows of the 377 DNA sequencer for the a) ABI dye set (FAM, JOE, TAMRA, and ROX) and b) dye-primers from cassettes **1–4** (DP **13–16**). Colored boxes indicate the four virtual filters, hatched regions represent nonimaged areas. Wavelength maxima for DP **13–16** were not centered relative to the virtual windows (see spectra in c)) because of the close clustering of cassettes **2**, **3**, and **4** (e.g., the emission maximum of cassette **3** differed by only 24 and 15 nm from that of cassettes **2** and **4**, respectively).

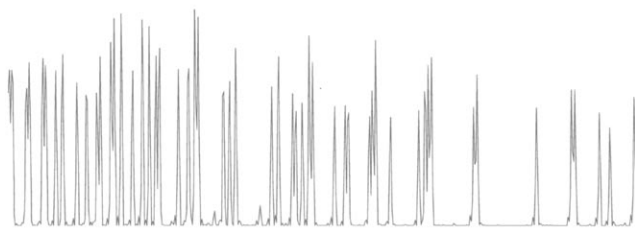
sequencing data can be obtained by using dye-primers from **1–4**. Unfortunately, it was not possible to obtain a set of the Big Dyes to compare their fluorescence intensities with cassettes **1–4**. The Big Dyes are precious materials; they are sold in relatively small quantities attached to DNA templates or 3'-deoxynucleoside triphosphate terminators.

Conclusion

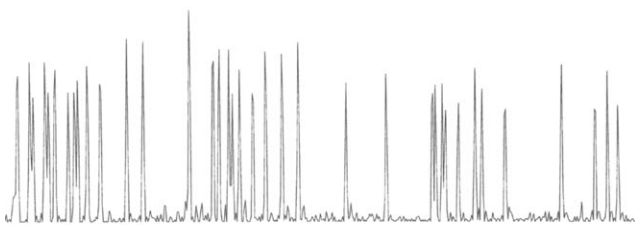
The state-of-the-art dyes for multiplexing applications in biotechnology tend to involve FRET donor-acceptor pairs that transfer energy by through-space energy mechanisms. This somewhat alleviates the loss of fluorescence intensity at longer wavelengths, as illustrated in Figure 1b, however, FRET-based cassettes are still limited by the requirement of overlap of the donor fluorescence with the acceptor absorbance. The same constraints do not appear to define the limits of through-bond energy transfer; hence, this mechanism can be exploited to generate cassettes with the same donor part, but with acceptor parts that emit strongly to the red.

The work described features the first through-bond energy-transfer cassettes for biotechnology constructed from fluorescein and rhodamine derivatives. Syntheses devised for these materials feature the preparation of specially de-

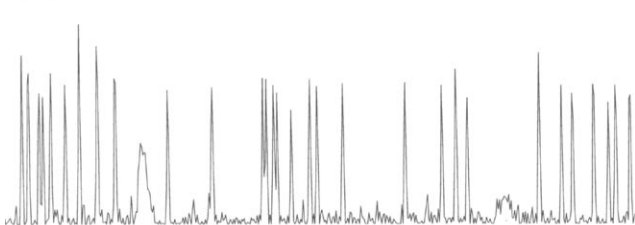
Dye-primer 13



Dye-primer 14



Dye-primer 15



Dye-primer 16

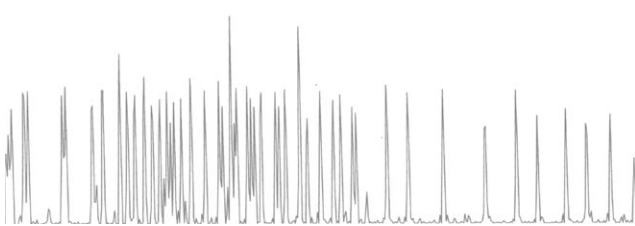


Figure 8. Single-nucleotide termination patterns for ddC, ddA, ddG, and ddT are represented in the diagrams for dye-primers 13–16, respectively. PCR products used as templates for the sequencing reactions were from HNF-1 α exon 10 for dye-primers 13–15, and from HNF-1 α exon 3 for dye-primer 16.

signed fluorescein- and rhodamine-derived synthons, followed by palladium-mediated coupling of these fragments by means of a convergent strategy. Upon exciting at around 490 nm, cassettes 1–4 emit strongly, even those featuring acceptors that fluoresce towards the red. Energy transfer in these systems is fast and efficient, faster than similar through-space energy-transfer cassettes, and the overall quantum yields of the cassettes are in the range 0.27–0.36. Direct application of the cassettes in automated dye-primer Sanger sequencing approaches is not straightforward, because adjustment of the software that enables differentiation of the four “color” outputs is problematic. Nevertheless, we have demonstrated the preliminary application of cassettes 1–4 in single-color sequencing experiments. We are continuing our work to design and prepare different types of through-bond energy-transfer probes for applications in biotechnology.

Acknowledgements

We would like to thank members of the TAMU/LBMS-Applications Laboratory directed by Dr. Shane Tichy for assistance with mass spectrometry. Support for this work was provided by The National Institutes of Health (HG 01745 and GM72041) and by The Robert A. Welch Foundation.

- [1] F. Sanger, A. R. Coulson, *J. Mol. Biol.* **1975**, *94*, 441–448.
- [2] F. Sanger, S. Nicklen, A. R. Coulson, *Proc. Natl. Acad. Sci. USA* **1977**, *74*, 5463–5467.
- [3] L. M. Smith, J. Z. Sanders, R. J. Kaiser, P. Hughes, C. Dodd, C. R. Connell, C. Heiner, S. B. Kent, L. E. Hood, *Nature* **1986**, *321*, 674–679.
- [4] T. Hunkapiller, R. J. Kaiser, B. F. Koop, L. Hood, *Science* **1991**, *254*, 59–67.
- [5] J. M. Prober, G. L. Trainor, R. J. Dam, F. W. Hobbs, C. W. Robertson, R. J. Zagursky, A. J. Cocuzza, M. A. Jensen, K. Baumeister, *Science* **1987**, *238*, 336–341.
- [6] T. Hunkapiller, R. J. Kaiser, B. F. Koop, L. Hood, *Anal. Biotechnol.* **1991**, *2*, 92–101.
- [7] R. A. Mathies, A. Glazer, J. Ju (Regents of the University of California, Oakland, CA, USA), US-5688648, **1997**.
- [8] L. G. Lee, M. C. Taing, B. B. Rosenblum (PE Corporation International), WO-02/36832 A2, **2002**.
- [9] L. G. Lee, B. Rosenblum, S. L. Spurgeon (Perkin-Elmer Corp.), US-EP805190 A, **1998**, p. 2.
- [10] B. B. Rosenblum, L. G. Lee, S. L. Spurgeon, S. H. Khan, S. M. Menchen, C. R. Heiner, S. M. Chen, *Nucleic Acids Res.* **1997**, *25*, 4500–4504.
- [11] L. G. Lee, S. L. Spurgeon, B. Rosenblum (Perkin-Elmer Corp.), US-EP0805190 A2, **1997**, p. 3.
- [12] L. G. Lee, S. L. Spurgeon, C. R. Heiner, S. C. Benson, B. B. Rosenblum, S. M. Menchen, R. J. Graham, A. Constantinescu, K. G. Upadhyaya, J. M. Cassel, *Nucleic Acids Res.* **1997**, *25*, 2816–2822.
- [13] J. R. Lakowicz, *Principles of Fluorescence Spectroscopy*, 2nd ed., Kluwer Academic/Plenum Publishers, New York, **1999**.
- [14] J. Ju, C. Ruan, C. W. Fuller, A. N. Glazer, R. A. Mathies, *Proc. Natl. Acad. Sci. USA* **1995**, *92*, 4347–4351.
- [15] J. Ju, I. Kheterpal, J. R. Scherer, C. Ruan, C. W. Fuller, A. N. Glazer, R. A. Mathies, *Anal. Biochem.* **1995**, *231*, 131–140.
- [16] M. L. Metzker, J. Lu, R. A. Gibbs, *Science* **1996**, *271*, 1420–1422.
- [17] S.-C. Hung, J. Ju, R. A. Mathies, A. N. Glazer, *Anal. Biochem.* **1996**, *238*, 165–170.
- [18] S.-C. Hung, J. Ju, R. A. Mathies, A. N. Glazer, *Anal. Biochem.* **1996**, *243*, 15–27.
- [19] J. Ju, A. N. Glazer, R. A. Mathies, *Nucleic Acids Res.* **1996**, *24*, 1144–1148.
- [20] J. Ju, A. N. Glazer, R. A. Mathies, *Nature Med.* **1996**, *2*, 246–249.
- [21] S.-C. Hung, R. M. Mathies, A. N. Glazer, *Anal. Biochem.* **1997**, *252*, 78–88.
- [22] R. A. Mathies, A. Glazer, J. Ju (Regents of the University of California, Oakland, CA, USA), US-5654419.
- [23] S. Hung, R. A. Mathies, A. N. Glazer, *Anal. Biochem.* **1998**, *255*, 32–38.
- [24] L. Berti, J. Xie, I. L. Medintz, A. N. Glazer, R. A. Mathies, *Anal. Biochem.* **2001**, *292*, 188–197.
- [25] L. Berti, I. L. Medintz, J. Tom, R. A. Mathies, *Bioconjugate Chem.* **2001**, *12*, 493–500.
- [26] L. Berti, J. Xie, I. L. Medintz, A. N. Glazer, R. A. Mathies, *Anal. Biochem.* **2001**, *292*, 188–197.
- [27] S. Nampalli, M. Khot, S. Kumar, *Tetrahedron Lett.* **2000**, *41*, 8867–8871.
- [28] S. Nampalli, W. Zhang, T. S. Rao, H. Xiao, L. P. Kotra, S. Kumar, *Tetrahedron Lett.* **2002**, *43*, 1999–2003.
- [29] S.-C. Hung, A. Glazer, R. A. Mathies (DNA Sciences, Fremont, CA, USA), US-6573047 B1, **2003**.

- [30] S.-I. Kawahara, T. Uchimar, S. Murata, *Chem. Commun.* **1999**, 563–564.
- [31] Y. Ohya, K. Yabuki, M. Hashimoto, A. Nakajima, T. Ouchi, *Bioconjugate Chem.* **2003**, *14*, 1057–1066.
- [32] A. K. Tong, S. Jockusch, Z. Li, H.-R. Zhu, D. L. Akins, N. J. Turro, J. Ju, *J. Am. Chem. Soc.* **2001**, *123*, 12923–12924.
- [33] A. K. Tong, Z. Li, G. S. Jones, J. J. Russo, J. Ju, *Nat. Biotechnol.* **2001**, *19*, 756–759.
- [34] A. K. Tong, J. Ju, *Nucleic Acids Res.* **2002**, *30*, 1–7.
- [35] J. M. Tour, *Chem. Rev.* **1996**, *96*, 537–553.
- [36] T. M. Swager, C. J. Gil, M. S. Wrighton, *J. Phys. Chem.* **1995**, *99*, 4886–4893.
- [37] C. Weder, M. S. Wrighton, *Macromolecules* **1996**, *29*, 5157–5165.
- [38] S. Speiser, *Chem. Rev.* **1996**, *96*, 1953–1976.
- [39] R. W. Wagner, J. S. Lindsey, *J. Am. Chem. Soc.* **1994**, *116*, 9759–9760.
- [40] F. Li, S. I. Yang, Y. Ciringh, J. Seth, C. H. Martin, D. L. Singh, D. Kim, R. R. Birge, D. F. Bocian, D. Holten, J. S. Lindsey, *J. Am. Chem. Soc.* **1998**, *120*, 10001–10017.
- [41] P. G. Van Patten, A. P. Shreve, J. S. Lindsey, R. J. Donohoe, *J. Phys. Chem. B* **1998**, *102*, 4209–4216.
- [42] M. S. Vollmer, F. Würthner, F. Effenberger, P. Emele, D. U. Meyer, T. Stümpfig, H. Port, H. C. Wolf, *Chem. Eur. J.* **1998**, *4*, 260–269.
- [43] K. Burgess, A. Burghart, J. Chen, C.-W. Wan in *SPIE BiOS 2000 The International Symposium on Biomedical Optics*: San Jose, CA, **2000**.
- [44] A. Burghart, L. H. Thoresen, J. Chen, K. Burgess, F. Bergström, L. B.-A. Johansson, *Chem. Commun.* **2000**, 2203–2204.
- [45] C.-W. Wan, A. Burghart, J. Chen, F. Bergstroem, L. B.-A. Johansson, M. F. Welford, T. G. Kim, M. R. Topp, R. M. Hochstrasser, K. Burgess, *Chem. Eur. J.* **2003**, *9*, 4430–4441.
- [46] S. H. Lin, W. Z. Xiao, W. Dietz, *Phys. Rev. E* **1993**, *47*, 3698–3706.
- [47] G.-S. Jiao, L. H. Thoresen, K. Burgess, *J. Am. Chem. Soc.* **2003**, *125*, 14668–14669.
- [48] G.-S. Jiao, J. W. Han, K. Burgess, *J. Org. Chem.* **2003**, *68*, 8264–8267.
- [49] G.-S. Jiao, J. C. Castro, L. H. Thoresen, K. Burgess, *Org. Lett.* **2003**, *5*, 3675–3677.
- [50] R. E. Kellogg, R. G. Bennett, *J. Chem. Phys.* **1964**, *41*, 3042–3045.
- [51] T. G. Kim, M. R. Topp, *J. Phys. Chem. A* **2004**, *108*, 10060–10065.
- [52] T. Wilhelm, J. Piel, E. Riedle, *Opt. Lett.* **1997**, *22*, 1494–1496.
- [53] H. Z. Yu, J. S. Baskin, A. H. Zewail, *J. Phys. Chem. A* **2002**, *106*, 9845–9854.
- [54] T. G. Kim, J. C. Castro, A. Loudet, J. G.-S. Jiao, R. M. Hochstrasser, K. Burgess, M. R. Topp, *J. Phys. Chem.* **2006**, *110*, 20–27.
- [55] P. G. Seybold, M. Gouterman, J. Callis, *Photochem. Photobiol.* **1969**, *9*, 229–242.
- [56] C. Eggeling, J. Widengren, R. Rigler, C. A. M. Seidel in *Appl. Fluoresc. Chem., Biol. Med.* **1999**, pp. 192–540.
- [57] M. A. Bopp, A. Sytnik, T. D. Howard, R. J. Cogdell, R. M. Hochstrasser, *Proc. Natl. Acad. Sci. USA* **1999**, *96*, 11271–11276.

Received: February 13, 2006
Published online: August 3, 2006